Effect of zinc and iron ions on the electrochemistry of nickel oxide electrode: slow cyclic voltammetry

Ivan Krejčí* and Petr Vanýsek
Northern Illinois University, Department of Chemistry, DeKalb, IL 60115-2862 (USA)

(Received February 16, 1993; accepted in revised form June 11, 1993)

Abstract

Porous nickel oxide electrodes were prepared by cathodic electroprecipitation from metal nitrate solutions on sintered substrate and characterized by slow (0.1 m V/s) voltammetry in 6 mol/l KOH. The presence of iron or zinc ions added to the electrolyte after formation of the electrodes resulted in a decrease of electrode charging ability. Removal of iron or zinc ions and presence of lithium ions partially restored the voltammogram to original conditions. Presence of cobalt in the electrode material diminished substantially the influence of zinc ions on the electrode properties.

Introduction

The nickel oxide electrode (NOE) has been investigated as a cathode suitable for electrochemical power sources since the times of Jungner and Edison [1–3]. Nickel/zinc and nickel/iron accumulators are attractive for traction purposes even today due to the cost and lifetime of the Ni/Fe accumulator, and due to the good peak power and high specific capacity of the Ni/Zn accumulator.

Nickel-based electrodes have a wide application. The nickel/metal hydride battery has been developed as an environmentally safe replacement for the nickel/cadmiun battery. Its high energy density, power, and cycle-life characteristics prompted subsequent development as a power source for electric vehicles [4, 5]. The nickel/hydrogen battery, originally introduced in space applications, has now also found terrestrial uses. It has a long cycle life, high specific energy, high reliability and good resilience to abuse, in particular to overcharge and polarity reversal. NOE is also used in fuel cells [6], electrolyzers [7], in organic electrosynthesis [8], and in electrolytic hydrogen production as an anode for oxygen evolution [9].

Various metallic additives have been examined in various battery systems [1, 3, 10–13] to modify the electrochemical properties of NOE to meet the need of specific applications [9]. Electrochemical measurements on nickel hydroxide thin films with chemically coprecipitated cobalt, iron and manganese [12, 14, 15] were performed several years ago. Electrochemistry of thin film binary composite hydroxide of nickel and 13 other metals using cyclic voltammetry in 1 mol/l KOH is described in ref. 10. A recent review on the nickel oxide electrode was presented by McBreen [16].

Cobalt and lithium additives improve the charge storage reaction and cycle-life time of nickel oxide electrode [1–3]. On the other hand, iron and zinc in the electrolyte

*On the leave from the J. Heyrovský Institute of Physical Chemistry and Electrochemistry, Academy of Sciences of the Czech Republic, Prague.

0378-7753/94/$07.00

decrease its charge storage ability, which in the case of iron is known as the iron poisoning effect [1, 10, 17]. However, zinc ions, when incorporated into the lattice structure, have been observed to improve the performance of porous nickel electrodes [18]. Better understanding of the effects of the main metallic additives and impurities on the electrochemistry of the nickel oxide electrode are important contributions to the battery industry.

Our study, that deals with effects of metal ions added to the electrolyte solutions, shows that some of the negative chemical effects of iron and zinc on nickel electrode performance can be alleviated by the presence of cobalt and lithium. The influence of iron and zinc on NOE performance under different conditions was studied in 6 mol/l KOH. Unlike experiments in which thin nickel hydroxide films were deposited on smooth electrode surfaces [10, 19], our studies were performed on a porous electrode from the same material which is encountered in actual power source applications. Because the diffusion of ions in the bulk of the porous electrode is slow, voltammetry at the usual scan rate ($\geqslant 5$ mV/s) yields distorted voltammograms with no developed peaks. Slow voltammetry (0.1 mV/s) in our work produced well developed peaks enabling a descriptive study of ion effects using the features of the voltammograms.

Experimental

The EG&G (Princeton Applied Research) 273 potentiostat/galvanostat was used to apply current and to control the potential during the experiments. The electrochemical cell was custom made. It was closed with a Teflon head through which all electrodes, nitrogen supply, and other accessories were introduced. Nickel foils on both sides of the porous nickel oxide working electrode were used as counter electrodes. A Hg/HgO reference electrode in 6 mol/l KOH had a contact with the working solution through a capillary 1 mm apart from the working electrode. It was separated from the working electrolyte by two frits to avoid contamination by added ions. All potentials, reported in this work, are given against this Hg/HgO electrode. Nitrogen was introduced in the cell prior and during the experiment.

The anodes were prepared by cathodic deposition of nickel hydroxide on commercially available SAFT (Poitiers, France) nickel sinter support (thickness: 0.7 mm, area: 1 cm^2) from aqueous 1 mol/l nickel nitrate solution or from a mixture of 1 mol/l nickel nitrate and 10 mmol/l cobalt nitrate. Spot-welded nickel wire was used as a current collector, nickel foil was used as a counter electrode. The nickel sinter was allowed to soak in the electrolyte for 30 min, before a current of 10 mA was applied at room temperature for 5 h, corresponding to the total loading capacity of 50 mAh. The electrodes were then rinsed in distilled water and dried in air at 55 °C for 3 h and the total amount of deposited active mass was determined; 0.038 g for electrode no. 1 and 0.026 g for no. 2. Dry electrodes were immersed before formation for 30 min in 6 mol/l KOH. The formation took place in a simple cell with a nickel counter electrode with formation charging and discharging current of 2 mA. The electrodes were charged to 150% of their capacity calculated from deposited active mass and discharged to 0.0 V. The discharging capacity was determined after the third formation cycle. The stability of response of the formed electrode was verified by performing several voltammetric cycles. Steady response was typically obtained after four to five cycles. The solutions were prepared from Fisher Certified A.C.S. chemicals and double-distilled water. Fisher Reagent KOH contained 0.0003% of iron and 0.0003% heavy metals (as silver). All experiments were performed at 24 ± 1 °C.

The electrodes were conditioned before each voltammetric experiment. After the last formation cycle a conditioning potential of either 500 or 550 mV, depending on the onset of oxygen evolution current, was applied for 1 h to stabilize the state-of-charge according to the type of the electrode and/or its history. The initial potential for voltammetry was either 550 or 600 mV, according ot oxygen evolution current. The sweep began negatively at 0.1 mV/s to 0.0 V, where the scan was reversed and continued to the starting potential.

An important feature on the voltammograms is the potential of oxygen evolution. For the purpose of this work, it was determined as the potential at which the oxygen anodic current drops below 40 mA during the negative sweep. The negative sweep was chosen because there was no interference from the NOE oxidation peak.

Results and discussion

Electrode prepared from nickel nitrate

Two electrodes, no. 1 and no. 2, were studied in this work. Electrode no. 1 was prepared by cathodic deposition from 1 mol/l $Ni(NO_3)_2$ solution. Electrode no. 2 contained in addition incorporated cobalt. Voltammograms obtained from eight experiments performed in sequence in various electrolytes with electrode no. 1 are given in Figs. 1 and 2 and important values describing the features of these voltammograms are given in Table 1.

Table 1 lists the potentials of reduction and oxidation peaks of nickel hydroxide, which are affected by the presence of metal ions. The average peak potential, as a measure of the reversible potential, and the peak potential separation, as a measure of degree of reversibility [10], were calculated. The separation of oxygen evolution (SOE) is a potential difference between the potential of oxygen evolution and the potential of the anodic peak. It is desirable that this value is high for power sources. It is a measure of electrode material ability to catalyze oxygen evolution:

$$4OH^- \longrightarrow O_2 + 2H_2O + 4e^- \quad (1)$$

Curve 1 is a voltammogram recorded during the third voltammetric sweep with the electrode conditioned only by formation cycles and charged. Addition of iron ions in the electrolyte (0.41 mmol/l $Fe(NO_3)_3$) resulted immediately in a change of the curve, particularly in its oxidation region (curve 2). The nickel hydroxide oxidation peak shifted positively about 10 mV, and the potential of oxygen evolution shifted negatively by about 20 mV. The SOE decreases to 47 mV in comparison with 84 mV for the electrode without iron (curve 1). The average peak potential shifted 10 mV positively and the peak potential separation remained the same. The subsequent voltammetric sweep (curve 3) reflects an even more pronounced effect of iron. Although the position of the oxidation peak remained the same, the oxygen evolution potential shifted further negatively. The SOE decreased to a mere 40 mV, which is nearly half the value for NOE without iron, and an example of the iron poisoning effect [17]. The average peak potential for curve 3 was only 15 mV more positive than for curve 1, and the peak potential separation decreased as previously reported [10].

After this voltammetric sweep, the electrode was washed in running distilled water to neutral reaction, and the cell was rinsed and refilled with KOH electrolyte containing 20 g/l LiOH. The peaks shifted negatively and the potential of oxygen evolution separation increased to 77 mV (curve 4). The average peak potential shifted negatively by 34 mV and the peak potential separation increased by 28 mV. These values are

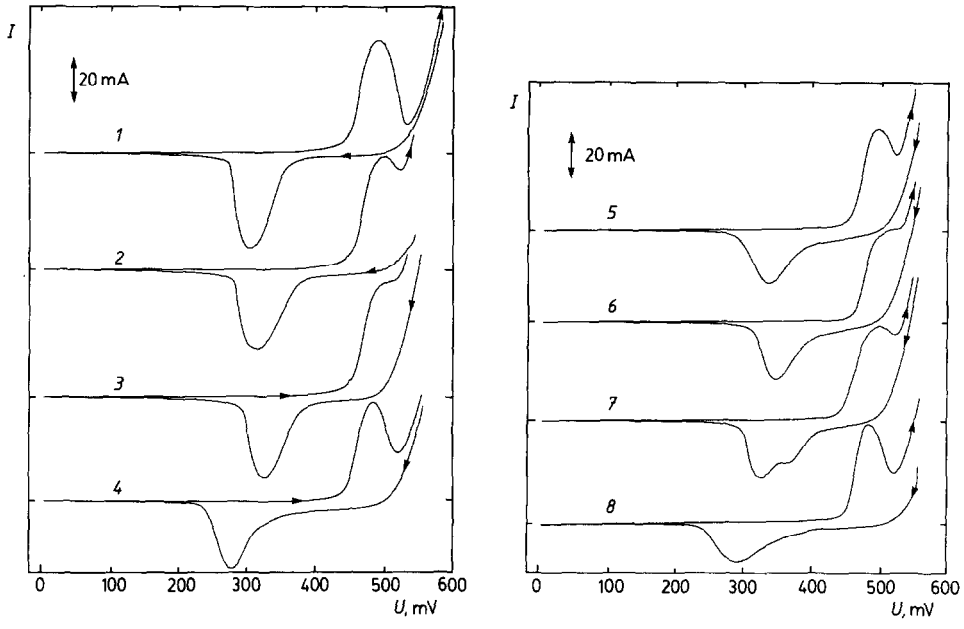

Fig. 1. Voltammograms for nickel oxide electrode no. 1, without cobalt, after formation cycles with various electrolyte compositions. Scan rate 0.1 mV/s: (1) 6 mol/l KOH; (2) 6 mol/l KOH + 0.41 mmol/l $Fe(NO_3)_3$; (3) next cycle following curve 2, the same electrolyte, and (4) 6 mol/l KOH + LiOH (20 g/l).

Fig. 2. Voltammograms for nickel oxide electrode no. 1, continuation of Fig. 1: (5) 6 mol/l KOH + 0.1 mol/l ZnO; (6) 6 mol/l KOH + 0.1 mol/l ZnO, sixth cycle after curve 5; (7) 6 mol/l KOH, after removing electrolyte with zinc ions, and (8) 6 mol/l KOH + LiOH (20 g/l).

TABLE 1

Values of the potentials of voltammetric features for electrode no. 1 with pure nickel hydroxide

1[a]	2	3	4	5	6	7	8	9
1	3	0	300	483	392	183	567	84
2	6	+Fe	310	493	402	183	540	47
3	7	Fe	320	493	407	173	533	40
4	9	−Fe, +Li	273	473	373	200	550	77
5	15	−Li, +Zn	330	488	409	158	550	62
6	21	Zn	342	500	421	158	535	35
7	23	−Zn	337	493	415	156	533	40
8	27	+Li	285	478	382	193	550	72

[a]Column 1: no. of the figure. Column 2: no. of the cycle. Column 3: addition or removal of the additives from electrolyte. Column 4: potential of the reduction peak (mV). Column 5: potential of the oxidation peak (mV). Column 6: average peak potential (mV). Column 7: oxidation/reduction peak potential separation (mV). Column 8: potential of oxygen evolution (mV). Column 9: separation of oxygen evolution SOE (difference between the oxidation peak potential and potential of the oxygen evolution) (mV).

larger than those for the fresh electrode, which was probably due to the combined effect of iron removal and the beneficial effect of lithium. The SOE did not, however, return to its previous value but its increase was significant. Traces of iron were obviously still either incorporated in the nickel hydroxide lattice or adsorbed on the surface and catalyzed the oxygen evolution. This influence of iron agrees with previous observations [10, 17], where the presence of iron and its incorporation in the matrix was confirmed by X-ray photoelectronspectroscopy (XPS).

An effect similar to iron poisoning resulted from the immersion of the electrode in a solution containing 6 mol/l KOH + 0.1 mol/l ZnO (curve 5). The potential of the oxidation peak in the first cycle after immersion in zinc containing solution increased and the potential of oxygen evolution remained the same, which decreased the SOE to 62 mV, which was 15 mV less than the values in absence of zinc (curve 4). The anodic peak began to deform in a similar way as in the presence of iron (curve 2). The average peak potential was 409 mV which agreed with ref. 10, and the peak potential separation decreased to 158 mV, compared with 200 mV in the presence of lithium. This lower value was likely caused by zinc in the lattice of nickel hydroxide. During the sixth voltammetric cycle in the same electrolyte the oxidation peak increased to 500 mV and the potential of oxygen evolution decreased to 535 mV, which resulted in SOE by only 35 mV (curve 6). It appears that prolonged exposure to zinc ions had the same effect on electrode no. 1 as iron ions. Comparison of the oxidation peaks on curves 5 and 6 with the peaks on curves 2 and 3 reveals this similarity.

In the following experiment the electrode was immersed into a solution of 6 mol/l KOH with no zinc present. The oxidation peak potential shifted 7 mV negatively and the potential of oxygen evolution remained nearly the same. The values of the average peak potential, the peak potential separation and SOE slowly shifted in the direction of the values obtained with the fresh electrode (curve 7, recorded during the second cycle after zinc removal).

Because restoration of the original values of potentials did not occur within the three cycles after zinc removal, the electrolyte was replaced by 6 mol/l KOH with LiOH, which is known to have a beneficial effect on NOE. After the next free cycles the potential of the oxidation peak reached 478 mV and potential of the oxygen evolution 550 mV, with SOE of 72 mV (curve 8). The average peak potential reached 382 mV, which was lower than that for the original electrode, but 10 mV higher than for the cycle after which iron ions were removed. The peak potential separation changed similarly. Separation of oxygen evolution was 12 mV lower than the original electrode value. Traces of iron were probably still able to partially decrease the potential of oxygen evolution. It should be noted that in this work independent chemical analysis of ion incorporation in the lattice was not performed. Our speculations are based on a previous study [17] that found by XPS that iron remains in the porous electrode for many polarization cycles.

Iron and zinc ions also had an influence on the position of the reduction peak. Both ions caused an increase of the reduction peak potential, and their removal returned the potential nearly to its previous value. All these results are summarized in Table 1.

Galvanostatic (E versus t) charging curves also were modified in the presence of iron [17] or zinc ions. Figure 3 presents galvanostatic curves for several stages in the experiment. Curve A corresponds to the pure nickel oxide electrode (no. 1) charged in 6 mol/l KOH. It shows a step on the curve that separates the potential of nickel hydroxide oxidation from the potential of oxygen evolution. In the presence of iron ions this step (potential separation) disappeared due to lower oxygen overvoltage which

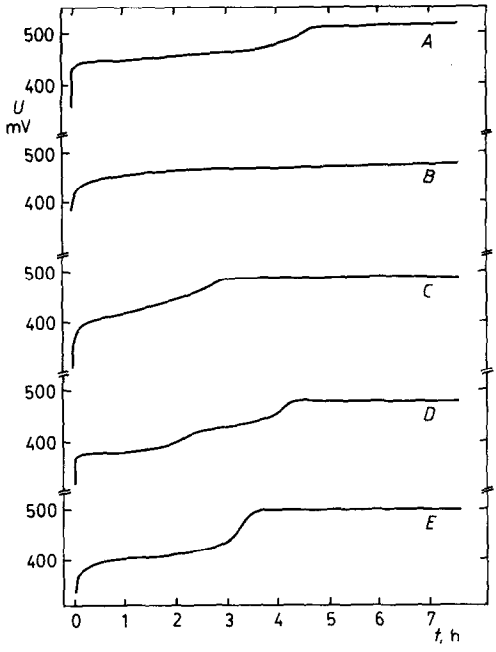

Fig. 3. Galvanostatic charging curves for electrode no. 1 without cobalt (A, B, C) and electrode no. 2 with cobalt (D, E): (A) 6 mol/l KOH, current 2 mA; (B) 6 mol/l KOH+0.1 mol/l ZnO, current 2 mA; (C) 6 mol/l KOH, current 2 mA, (D) 6 mol/l KOH, current 2 mA, and (E) 6 mol/l KOH+0.1 mol/l ZnO, current 3 mA.

TABLE 2

Discharge capacities and charging potentials of electrode no. 1 with pure nickel hydroxide[a]

Electrolyte composition	Discharge capacity (mAh)	Potential (mV)	Curve in Fig. 3
KOH	9.5	514	A
KOH+Fe	6.5	480	
KOH+Li	8.5	510	
KOH+Zn	5.4	475	B
KOH	6.0	490	C
KOH+Li	7.0	490	

[a]The capacity was measured at 2 mA, discharging to 0.0 V vs. Hg/HgO. Charging potential is the NOE potential at the end of charging to 150% capacity by 2 mA. The electrode was always conditioned by discharging to 0.0 V before recording the charging and discharging curves.

resulted in low charging efficiency of the electrode, a lower end-of-charge potential and decreased discharging capacity, a behavior also reported previously [17]. Removing the electrode from the environment with iron ions restored the shape of the charging curve, increased the end potential and partially increased the discharging capacity. This was more pronounced in the presence of lithium, as was also reported previously [17]. The capacities and charging potentials of electrode no. 1 are given in Table 2

Changes of the galvanostatic charging curve and loss of the discharging capacity similar to those caused by iron ions were also observed in the presence of zinc ions (curve B and Table 2). The end potential of charging was 475 mV, 39 mV lower than that for a fresh electrode and very similar to 480 mV in the presence of iron. Discharging capacity was 5.4 mAh in comparison with 6.5 mAh for the electrode with iron, and 9.5 mAh for the fresh electrode. It should be noted that these low values for zinc can be caused by traces of iron incorporated in the lattice of the nickel hydroxide during the previous experiment.

Placing the electrode into a new electrolyte (6 mol/l KOH) without zinc ions increased the discharging capacity and the potential at the end of charging (Fig. 3, curve C). Addition of 20 g/l LiOH caused an additional increase of the discharging capacity, but the shape of the charging curve and the end-of-charging potential remained the same. Traces of iron or zinc incorporated inside the nickel hydroxide lattice could obviously catalyze oxygen evolution as a reaction parasitic to the charging process.

Electrode prepared from nickel nitrate with cobalt

To study the influence of cobalt, electrode no. 2 was prepared in a way similar to electrode no. 1, by cathodic deposition from aqueous solution of 1 mol/l $Ni(NO_3)_2$ and 0.01 mol/l $Co(NO_3)_2$. The resulting voltammograms are shown in Fig. 4 and their significant features are listed in Table 3. Perusal of the curves reveals that cobalt has a significant influence. Curve 9 is a voltammogram of a freshly prepared electrode after three formation and three voltammetric cycles in 6 mol/l KOH. Potentials of the oxidation and reduction peaks were lower than those for an electrode without cobalt, and the potential of oxygen evolution was higher. The negative shift of the reduction peak was about 14 mV, which is less than the previously reported

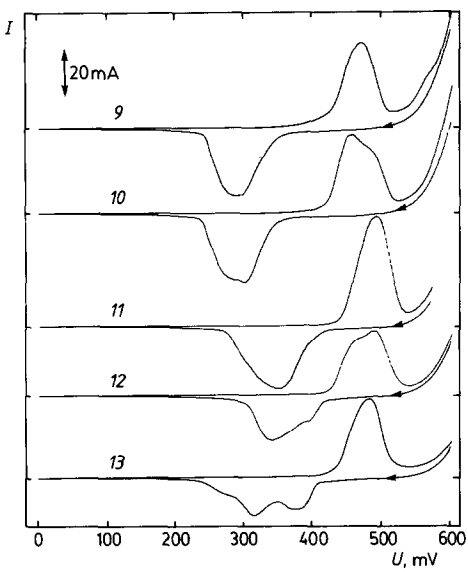

Fig. 4. Voltammograms for nickel oxide electrode no. 2, with cobalt, with different electrolyte compositions. Scan rate 0.1 mV/s: (9) 6 mol/l KOH; (10) 6 mol/l KOH + 0.1 mol/l ZnO; (11) 6 mol/l KOH + 0.1 mol/l ZnO, 8th cycle after curve 10; (12) 6 mol/l KOH, and (13) 6 mol/l KOH + LiOH (20 g/l).

TABLE 3

Values of the potentials of voltammetric features for electrode no. 2 with added cobalt in nickel hydroxide

1[a]	2	3	4	5	6	7	8	9
9	4	0	286	468	377	182	600	132
10	5	+Zn	288	468	378	180	603	135
11	13	Zn	347	488	418	141	613	125
12	30	−Zn	338	481	410	143	605	130
13	36	+Li	313	478	396	165	615	137

[a]Column 1: no. of the figure. Column 2: no. of the cycle. Column 3: addition or removing of the additives. Column 4: potential of the reduction peak (mV). Column 5: potential of the oxidation peak (mV). Column 6: average peak potential (mV). Column 7: oxidation/reduction peak potential separation (mV). Column 8: potential of oxygen evolution (mV). Column 9: separation of oxygen evolution SOE (difference between the potential of the oxidation peak and potential of oxygen evolution) (mV).

100 mV [20]. It is probably due to the same reason as reported in ref. 10, namely lower concentration of cobalt. Also, the starting nickel hydroxide in our case was the α, rather than the β phase. While charge/discharge cycle generally converts α to β, the history of the electrode may still be important. Curve 10 depicts the voltammetric response immediately after addition of the zinc ions. During the first voltammetric cycle, all the voltammetric features were nearly the same as for an electrode without zinc, only the peaks were somewhat broader.

The situation changed after seven voltammetric cycles (curve 11). Oxidation and reduction peaks shifted positively by 20 and 61 mV, respectively, which resulted in a decrease of the peak potential separation. The separation of oxygen evolution was about 10 mV lower than in curve 10. The average peak potential shifted positively 41 mV, which corresponded well with ref. 10. Replacement of the electrolyte by 6 mol/l KOH without zinc ions (curve 12) shifted the potentials somewhat towards the original electrode values.

Curve 13 in Fig. 4 is a fourth voltammetric cycle after adding LiOH to the electrolyte. The oxidation and reduction peaks continued to shift towards the value for the original electrode, but did not reach them. The average peak potential was still about 20 mV greater than for curve 9. There was a significant change in potential of the oxygen evolution, which was 15 mV higher than the original value. Thus, SOE reached 137 mV.

The values of SOE for the electrode with cobalt are significantly higher in all experiments than the corresponding values for an electrode without cobalt. The known beneficial effect of the cobalt on SOE from the nickel hydroxide oxidation seems to remain even in the presence of some amount of zinc. A puzzling feature is the shape of the reduction peak on curve 13. The reduction peaks in the presence of zinc (curves 10, 11) or after removing zinc ions (curves 7, 12) have the tendency to broaden or to split, which was not observed in ref. 10. Broadening of reduction peaks is known in the case of ternary metal hydroxide electrodes [19].

Galvanostatic charging curves were recorded for electrode no. 2 after formation in electrolyte without zinc (Fig. 3, curve D) and after ten voltammetric cycles in the presence of zinc ions (curve E). Associated calculated values for these curves are given in Table 4. There were two steps on the charging curve D for electrode no. 2

TABLE 4

Discharge capacities and the charging potential for electrode no. 2 with added cobalt in nickel hydroxide

Electrolyte composition	Discharge capacity (mAh)	Potential (mV)	Curve in Fig. 3
KOH	7.2	485	D
KOH+Zn	6.5[a]	503	E

[a]Charging current 3 mA, discharging current 5 mA. Other comments the same as for Table 2.

in 6 mol/l KOH, which is common for electrodes with cobalt added. The lower initial capacity of this electrode in comparison with the value for electrode no. 1 without cobalt is due to the lower amount of active mass. Curve E illustrates the situation after several voltammetric cycles in the presence of the zinc ions. One of the steps disappeared and the end potential of charging increased due to the influence of zinc ions in the presence of cobalt. Addition of zinc lowered the discharging capacity, but only by about 10%, in comparison with the 35% observed for the electrode without cobalt. This shows that in the presence of cobalt, zinc does not have the same detrimental effect on the charging ability.

Conclusions

While most authors [10, 15, 19, 20] have studied the effect of doping NOE by other cations on thin hydroxide films deposited on platinum, this work was done on a porous thick substrate. Insertion or iron and zinc ions from a solution into the porous structure on nickel provided results not available in other ways. The results were achieved by very slow voltammetric scans (0.1 mV/s). Because of the duration of a single cycle and the number of cycles performed on each electrode (27 and 36, respectively), the results provide data about electrodes under long-term study.

The effect of zinc and of iron on the electrode prepared with pure nickel hydroxide were very similar, including the partial restoration of electrode properties once these ions were removed from the solution. The presence of cobalt in the electrode materials diminished the effect of zinc observed in electrodes without cobalt. Cobalt also increased the reversibility of the electrochemical reaction. It was observed that zinc in the cobalt-doped electrode even somewhat increased SOE. This could be used for inhibition of the parasitic oxygen evolution reaction to improve the charging efficiency of the nickel oxide electrodes in power sources. No oxidation peak of cobalt was observed at the 1% concentration, although at higher concentrations it can appear [14]. The absence of an oxidation peak has been previously confirmed [10, 15].

The value of the negative shift of the reduction peak for 1% cobalt is lower than otherwise reported 100 mV [20]. This is consistent with data in ref. 10. Whereas in work by Pickett and Maloy [20] the electrode material was β-$Ni(OH)_2$ and cobalt concentration was 10%, in our case the cobalt was codeposited from a 1% solution in an electrode which was originally α-$Ni(OH)_2$.

It is known that both the amount and the method of introduction of foreign cations in the nickel oxide electrode is important [17] as well as is the mutual ratio of the metal additives, their ratio to nickel hydroxide and their location in the structure

of nickel hydroxide [19]. This can be the reason why zinc with traces of iron had a detrimental effect on the NOE without cobalt, while the electrode made with added cobalt was hardly affected. Zinc actually appeared to have a small beneficial effect on the cobalt-containing electrode.

The peculiar splitting of the reduction peak or appearance of other redox reaction accompanying removal of the electrode from the medium with foreign cations is not understood, but is possibly caused by formation of a different phase of nickel hydroxide. More work is needed to evaluate the coeffect of different additives on NOE. In particular, trace analysis of the imbedded electrode components at individual stages of the experiment would be desired. Also, other phases of $Ni(OH)_2$ starting material, mainly β, which were not investigated in this work, should be studied in the presence of coadditives.

Acknowledgements

We thank Professor Giovanni Davolio (University of Modena, Italy) for samples of the nickel sinter support and for his helpful comments. The postdoctoral leave of I.K. was supported by the Office of Naval Research.

References

1 S.U. Falk and A.J. Salkind, *Alkaline Storage Batteries,* Wiley, New York, 1969.
2 D.H. Fritts, *J. Electrochem. Soc., 129* (1982) 118–22.
3 B. Klápště, K. Micka, J. Mrha and J. Vondrák, *J. Power Sources, 8* (1982) 351–357.
4 S.R. Ovshinsky, S. Venkatesan, M. Fetcenko and S. Dhar, *Proc. 24th Symp. Automotive Technology and Automation, Florence, Italy, May 1991.*
5 S. Venkatesan, M.A. Fetcenko, D.A. Corrigan, S.K. Dhar and S.R. Ovshinsky, *182nd Meet. Electrochemical Society, Toronto, Canada, Oct. 11–16, 1992,* Paper No. 13.
6 F.T. Bacon, *J. Electrochem. Soc., 126* (1979) 7C–17C.
7 D.E. Hall, *J. Electrochem. Soc., 130* (1983) 317–321.
8 K. Manandar and D. Pletcher, *J. Appl. Electrochem., 9* (1979) 707–714.
9 D.A. Corrigan, *J. Electrochem. Soc., 134* (1987) 377–384.
10 D.A. Corrigan and R.M. Bendert, *J. Electrochem. Soc., 136* (1989) 723–728.
11 E.J. Casey, A.R. Dubois, P.E. Lake and W.J. Moroz, *J. Electrochem. Soc., 112* (1965) 371–375.
12 R.J. Doran, *Proc. 3rd Int. Symp. Batteries,* Admiralty Engineering Laboratories, West Drayton, UK, 1962, p. 105.
13 M. Oshitani, T. Takayama, K. Takashima and S. Tsuji, *J. Appl. Electrochem., 16* (1986) 403–411.
14 S.I. Cordoba, R.E. Carbonio, M. Lopez Teijelo and V.A. Macagno, *Electrochim. Acta, 31* (1986) 132–1332.
15 M.E. Folquer, J.R. Vilche and A.J. Arvia, *J. Electroanal. Chem., 172* (1984) 235–253.
16 J. McBreen, in R.E. White, J.O'M. Bockris and B.E. Conway (eds.), *Modern Aspects of Electrochemistry,* Vol. 21, Plenum, New York, 1990, Ch. 2, pp. 29–63.
17 I. Krejčí, J. Mrha, B. Folkesson and R. Larsson, *J. Power Sources, 21* (1987) 77–90.
18 D.H. Fritts, in R.G. Gunther and S. Gross (eds.), *Proc. Symp. on the Nickel Electrode,* Vol. 82-4, The Electrochemical Society, Pennington, NJ, USA, 1982, p. 175.
19 M.E. Uñates, M.E. Folquer, J.R. Vilche and A.J. Arvia, *J. Electrochem. Soc., 139* (1992) 2697–2704.
20 D.F. Pickett and J.T. Maloy, *J. Electrochem. Soc., 125* (1978) 1026–1032.